PHYSICAL REVIEW C **71**, 041302(R) (2005)

Reduced transition probabilities to the first 2^+ state in ^{52,54,56}Ti and development of shell closures at $N = 32, 34$

D.-C. Dinca,[1,2] R. V. F. Janssens,[3] A. Gade,[2] D. Bazin,[2] R. Broda,[4] B. A. Brown,[1,2] C. M. Campbell,[1,2] M. P. Carpenter,[3] P. Chowdhury,[3,5] J. M. Cook,[1,2] A. N. Deacon,[6] B. Fornal,[4] S. J. Freeman,[6] T. Glasmacher,[1,2] M. Honma,[7] F. G. Kondev,[8] J.-L. Lecouey,[2] S. N. Liddick,[2,9] P. F. Mantica,[2,9] W. F. Mueller,[2] H. Olliver,[1,2] T. Otsuka,[10] J. R. Terry,[1,2] B. A. Tomlin,[2,9] and K. Yoneda[2]

[1]*Department of Physics and Astronomy, Michigan State University, East Lansing, Michigan 48824*
[2]*National Superconducting Cyclotron Laboratory, Michigan State University, East Lansing, Michigan 48824*
[3]*Physics Division, Argonne National Laboratory, Argonne, Illinois 60439*
[4]*Institute of Nuclear Physics, Polish Academy of Sciences, PL-31342 Cracow, Poland*
[5]*University of Massachusetts Lowell, Lowell, Massachusetts 01854*
[6]*Department of Physics and Astronomy, Schuster Laboratory, University of Manchester, Manchester M13 9PL, United Kingdom*
[7]*Center for Mathematical Sciences, University of Aizu, Tsuruga, Ikki-machi, Aizu-Wakamatsu, Fukushima 965-8580, Japan*
[8]*Nuclear Engineering Division, Argonne National Laboratory, Argonne, Illinois 60439*
[9]*Department of Chemistry, Michigan State University, East Lansing, Michigan 48824*
[10]*Department of Physics and Center for Nuclear Study, University of Tokyo, Hongo, Tokyo 113-0033, Japan and RIKEN, Hirosawa, Wako-shi, Saitama 351-0198, Japan*

(Received 8 November 2004; published 15 April 2005)

The even $^{52-56}$Ti isotopes have been studied with intermediate-energy Coulomb excitation and absolute $B(E2; 0^+ \rightarrow 2_1^+)$ transition rates have been obtained. These data confirm the presence of a subshell closure at neutron number $N = 32$ in neutron-rich nuclei above the doubly magic nucleus ^{48}Ca and provide no direct evidence for the predicted $N = 34$ closure. Large-scale shell model calculations with the most recent effective interactions are unable to reproduce the magnitude of the measured strengths in the semimagic Ti nuclei and their strong variation with neutron number.

DOI: 10.1103/PhysRevC.71.041302 PACS number(s): 23.20.Js, 21.60.Cs, 25.70.De, 27.40.+z

Shell structure is the foundation for much of our present understanding of atomic nuclei, although most of our knowledge about the ordering and location in energy of the single-particle states remains empirical. In this context, neutron-rich nuclei have become the focus of recent theoretical and experimental efforts. The ongoing investigations are motivated to a large extent by expectations of substantial modifications of shell structure in nuclei with a sizable neutron excess [1]. Such alterations can have a considerable impact on global nuclear properties such as the nuclear shape or the type of excitations characterizing the low-energy level spectra. One of the proposed causes for the reordering of single-particle states is the proton-neutron monopole interaction [2]. This interaction has recently been invoked to account for the presence of a subshell gap at $N = 32$ in neutron-rich nuclei located in the vicinity of doubly magic $^{48}_{20}Ca_{28}$. At present, experimental evidence for the presence of this $N = 32$ gap rests solely on the low- and medium-spin ($I \leqslant 12$) level sequences of the ^{52}Ca [3], $^{52-56}$Ti [4–6], and $^{52-58}$Cr [7] even-even isotopes.

The purpose of this Rapid Communication is to track the evolution of this subshell gap further, through the measurement of the electromagnetic transition rates to the first excited states of the ^{52,54,56}Ti isotopes with the technique of intermediate-energy Coulomb excitation [8]. Such rates provide one of the most sensitive probes of nuclear structure. In deformed nuclei, transition strengths are related to the magnitude of the deformation, whereas in nuclei in the vicinity of closed shells, they are of great value in probing the details of the many-body wave functions. In fact, these rates have often highlighted properties that were unexpected on the basis of level energies alone. For example, the $B(E2; 0^+ \rightarrow 2_1^+)$ value in doubly magic ^{56}Ni was found to be larger than anticipated [9], whereas that measured for ^{136}Te, with two protons and two neutrons outside the doubly magic ^{132}Sn nucleus, is surprisingly small [10].

In the particular case discussed here, the transition rates represent a sensitive test of the most modern effective interactions that have been developed to describe *pf*-shell nuclei [11]. It is shown that the data support the view of a sizable shell gap at $N = 32$, but that there is no experimental evidence for an additional subshell closure predicted to occur at $N = 34$. Moreover, detailed comparisons between the data and the calculations also indicate shortcomings of the proposed effective interactions in reproducing the observed trend of the $B(E2)$ values with neutron number.

The measurements were carried out at the Coupled Cyclotron Facility of the National Superconducting Cyclotron Laboratory (NSCL) using secondary beams produced in fragmentation of ^{76}Ge at an energy of 130 MeV/nucleon. Following the 380 mg/cm^2 ^{9}Be fragmentation target, the species of interest were selected with the A1900 fragment separator [12] and directed to the target position of the high-resolution S800 magnetic spectrograph [13]. Four settings of the A1900 separator were used in the experiment. First, the ^{76}Ge primary beam was degraded to 81 MeV/nucleon

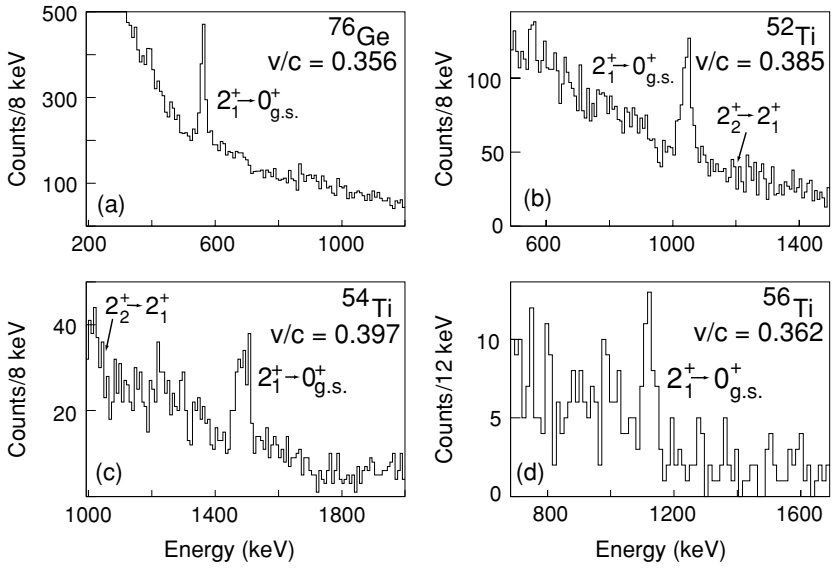

FIG. 1. Representative coincidence γ-ray spectra for ^{76}Ge and the even $^{52-56}$Ti isotopes Doppler reconstructed event by event in the projectile frame. The energy at mid-target for ^{76}Ge was 73.5 MeV/nucleon, and the distance of closest approach was 17.6 fm as deduced from the maximum scattering angle in the center-of-mass frame of projectile and target, $\theta_{\text{c.m.}} < 3.1^\circ$. For ^{52}Ti the corresponding values for the 256 mg/cm^2 and 518 mg/cm^2 Au targets were 82.4 and 79.1 MeV/nucleon, respectively, with $\theta_{\text{c.m.}} < 3.1^\circ$ and $<3.3^\circ$ and similar distances of closest approach of 13.9 fm. The spectrum measured with the thinner target is shown in the figure. For ^{54}Ti and ^{56}Ti, the respective projectile energies were 83.3 and 78.6 MeV/nucleon, with distances of closest approach of 14.0 fm and 14.1 fm computed from $\theta_{\text{c.m.}} < 3.2^\circ$ and $<3.6^\circ$. The arrows indicate the expected location of transitions deexciting the 2_2^+ levels (see text for details).

and sent onto a 256 mg/cm^2 ^{197}Au target as a check of the technique. Following this measurement, secondary beams of the three even Ti isotopes of interest, all with an energy of 89 MeV/nucleon, were then selected in succession and directed onto ^{197}Au targets of 256 and 518 mg/cm^2 thickness. The thinner Au target was used with the ^{52}Ti and ^{54}Ti fragments, and the thicker one with ^{52}Ti and ^{56}Ti. For a primary beam intensity of 10 pnA, the three Ti settings resulted in average rates on target of 9000 Hz (^{52}Ti), 600 Hz (^{54}Ti), and 40 Hz (^{56}Ti). Each incoming beam particle was identified on an event-by-event basis, and the isotopes of interest represented respectively 58, 28, and 10% of the flux of selected particles.

The Au target was surrounded by SeGA, an array of fifteen 32-fold segmented, germanium detectors [14] arranged in two rings with central angles of 90° and 37° relative to the beam axis. The forward ring contained seven detectors; the other eight were located at 90°. The high degree of segmentation is necessary to correct for the Doppler shift of the γ rays emitted in flight (on an event-by-event basis). Simulations with the code GEANT3 [15] reproduced the efficiency of SeGA measured with sources and provided the detector response for the in-beam data by taking into account the Lorentz boost (see Ref. [16] for further details). This reference also describes the particle identification and the determination of the scattering angle carried out on an event-by-event basis with the focal plane detector system [17] of the S800 spectrograph.

As already stated, inelastic scattering of the primary ^{76}Ge beam on the ^{197}Au target was used to validate the experimental technique. In ^{76}Ge, the reduced transition probability has been determined through Coulomb excitation at energies below the Coulomb barrier [18]. Figure 1(a) gives the relevant spectrum measured in the projectile frame for scattering angles restricting the impact parameter of the reaction to values larger than the sum of the two nuclear radii plus 5 fm. Using the Winther-Alder theory of relativistic Coulomb excitation [19], the angle-integrated cross section measured under these conditions translates into a value $B(E2; 0^+ \rightarrow 2_1^+) = 2923(346)\, e^2\text{fm}^4$ that compares well with the adopted one of 2780(30) e^2fm^4 [18]. From the same measurement, a similar comparison can be made for the excitation of the Au target and good agreement is again found between the present data and the literature [20]: $B(E2; 3/2^+ \rightarrow 7/2^+) =$ 4472(951) versus 4494(409) e^2fm^4.

With the reliability of the technique demonstrated, attention can now turn to the three even-mass Ti isotopes of interest. The analysis was carried out following the same prescription given for ^{76}Ge. In each case, the cross section for the excitation of the first 2^+ level was extracted from the γ-ray yields measured in spectra corrected for the Doppler shift and the response of the SeGA detectors (representative spectra for which are shown in Fig. 1), with appropriate restrictions on the scattering angle of the Ti fragments (see previous discussion and Ref. [16]). Table I presents the derived $B(E2; 0^+ \rightarrow 2_1^+)$ values. In the

TABLE I. Comparison of measured $B(E2; 0^+ \rightarrow 2_1^+)$ values [labeled $B(E2; \uparrow)$ in the table] with shell-model calculations using the GXPF1 interaction as well as the recently proposed GXPF1A interaction. The two ^{52}Ti entries correspond to separate measurements with Au targets of different thicknesses: (a) 256 mg/cm^2, (b) 518 mg/cm^2, and (c) the weighted average of the two. Data on the excitation of the Au target by the various Ti isotopes are given as well.

Nucleus	$B(E2;\uparrow)$ (e^2fm^4) expt.	$B(E2;\uparrow)$ (e^2fm^4) GXPF1	$B(E2;\uparrow)$ (e^2fm^4) GXPF1A	$B(E2;\uparrow)$ (e^2fm^4) 547 keV Au
^{52}Ti [(a)]	593(80)	427	435	4114(627)
^{52}Ti [(b)]	548(70)	427	435	4063(455)
^{52}Ti [(c)]	567(51)	427	435	
^{54}Ti	357(63)	453	446	4279(672)
^{56}Ti	599(197)	483	448	6356(2227)

case of ^{52}Ti, measurements were carried out with two targets of different thickness to ensure the validity of the experimental approach when thicker targets are required to compensate for lower fragment yields, as is the case here for ^{56}Ti. The two ^{52}Ti data points are in excellent agreement (Table I). Furthermore, they also agree with an earlier measurement [21], albeit the errors are large: $B(E2; 0^+ \rightarrow 2_1^+) = 665^{+515}_{-415}\, e^2\text{fm}^4$. Additional confidence in the transition rates of Table I comes from the data gathered simultaneously for Coulomb excitation of the target: The $B(E2; 3/2^+ \rightarrow 7/2^+)$ values for the excitation of ^{197}Au agree with each other and with the adopted value [20] (see Table I).

The values in Table I assume that the excitation of the 2_1^+ levels of interest occurs in a one-step, direct process without significant contribution(s) from higher lying 2^+ states to the measured $2_1^+ \rightarrow 0^+$ γ-ray yields. In ^{52}Ti, a number of such higher 2^+ states are known [22], and a 2_2^+ level has also been proposed tentatively in ^{54}Ti [4]. In the data for both nuclei, none of the γ rays associated with decays from these levels toward the ground state and the yrast 2_1^+ level were observed, as illustrated in Fig. 1 where the location of the $2_2^+ \rightarrow 2_1^+$ transitions in ^{52,54}Ti is given with arrows. The absence of peaks indicates that any feeding correction must be small. Furthermore, as discussed in the following, these excited levels are understood in the context of the shell model and the associated reduced transition probabilities are calculated to be smaller by an order of magnitude or more than the $B(E2; 0^+ \rightarrow 2_1^+)$ values under discussion here. The largest such strengths is predicted to occur for the 2_2^+ level in ^{52}Ti. In this case, the upper limit for the $2_2^+ \rightarrow 2_1^+$ intensity obtained from the data translates into a maximum correction to the $B(E2; 0^+ \rightarrow 2_1^+)$ value of 34 $e^2\text{fm}^4$ (i.e., well within the error bars of Table I). In all other cases the contributions from higher 2^+ levels would be even smaller and it is concluded that possible feeding corrections do not affect the values of Table I significantly.

Experimental evidence for a shell closure is usually inferred from at least two observables derived from nuclear spectra: the energy of the first excited state and the reduced transition probability to the same level. The former is expected to be rather large, reflecting the sizable energy gap associated with a shell or subshell closure, and the latter is anticipated to be small and comparable to single-particle estimates. Figure 2 presents the two physical quantities of interest for all even Ti isotopes with mass $A = 48$–56. From the figure, a clear anticorrelation between the two observables can be readily seen: whereas the $E(2_1^+)$ energies increase significantly at $N = 28$ and $N = 32$ [Fig. 2(a)], the $B(E2; \uparrow)$ strengths are lowest for these two neutron numbers [Fig. 2(b)]. Furthermore, both these physical quantities also differ markedly from the corresponding values at neutron numbers $N = 26$, 30, and 34. For ^{50}Ti, the well-known shell closure at $N = 28$ translates into a small transition probability: With the $B(E2)$ value of Fig. 2(b), the deexcitation from the 2_1^+ level to the ground state has a strength of only 5.6 single-particle units. The fact that the excitation energy and the reduced transition probability observed in ^{54}Ti are comparable to those in ^{50}Ti [see Fig. 2(b) and Table I] then suggests that the Ti isotope with $N = 32$ is as good a semimagic nucleus as its $N = 28$ counterpart and, hence, that a substantial subshell

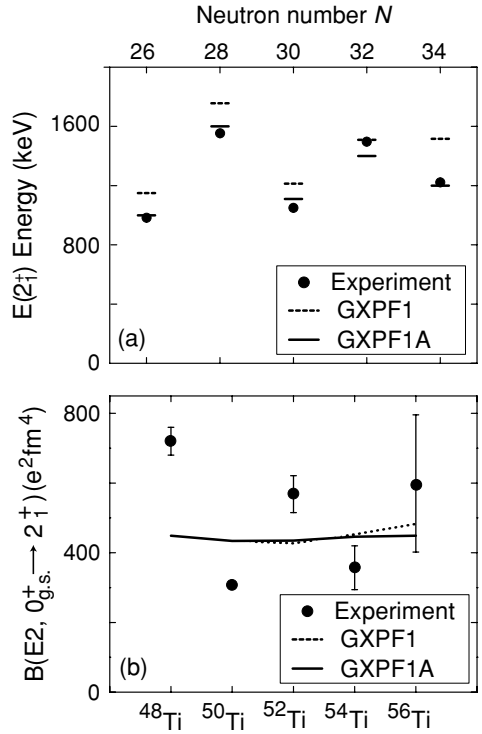

FIG. 2. Comparison of the measured 2_1^+ excitation energies and absolute $B(E2; 0^+ \rightarrow 2_1^+)$ transition strengths with the results of large-scale shell model calculations using the GXPF1 [dashed lines in panels (a) and (b)] and GXPF1A [solid lines in (a) and (b)] effective interactions. The $B(E2; 0^+ \rightarrow 2_1^+)$ value for ^{52}Ti is the weighted average of the two measurements given in Table I.

gap must occur at $N = 32$. Conversely, the fact that the three other Ti isotopes have 2_1^+ excitation energies lower by several hundreds of keV and $B(E2; 0^+ \rightarrow 2_1^+)$ values higher by a factor of $\sim$2 can be interpreted as an experimental indication for the absence of subshell gaps in the neutron single-particle spectrum at $N = 26$, 30, and 34.

Large-scale shell model calculations with the GXPF1 effective interaction, optimized for the description of *pf*-shell nuclei [11], attribute the onset of a $N = 32$ gap in neutron-rich Ca, Ti, and Cr nuclei to the combined actions of the $2p_{1/2}$-$2p_{3/2}$ spin-orbit splitting and the weakening of the monopole interaction strength between $f_{7/2}$ protons and $f_{5/2}$ neutrons. The dashed lines in Fig. 2(a) represent the results of calculations with this interaction: Although the $N = 32$ gap in the Ti isotopes is accounted for, the calculations also predict an additional gap at $N = 34$ that is not borne out by experiment. As pointed out in Refs. [5,6], the data suggest instead that the energy spacings among the $p_{3/2}$, $p_{1/2}$, and $f_{5/2}$ neutron orbitals, as well as the degree of admixture between these states in the wave functions of the ^{56}Ti yrast excitations, require further theoretical investigation. This has been done recently by Honma *et al.* [23] with the introduction of a modified version of the interaction, labeled GXPF1A, in which the matrix elements of the interaction involving mostly the $p_{1/2}$ orbital have been readjusted. It is worth pointing out that the evaluation of the properties of this orbital from experimental data is particularly challenging since it

contributes little angular momentum to any given state. Traces of its impact are often obscured as a result. The solid lines in Fig. 2(a) indicate that the GXPF1A calculations reproduce the $E(2_1^+)$ energies. In fact, they provide a satisfactory description of all the known levels in the even Ti nuclei, including those above the 6^+ level in ^{54}Ti, which involve neutron excitations across the $N = 32$ shell gap [23]. They also describe the odd Ti nuclei satisfactorily [24].

For all the even Ti isotopes, the wave functions of the 2^+ levels are dominated by $(f_{7/2})^2$ proton configurations coupled to ground and excited states of the neutron configurations. This is reflected in the proton and neutron amplitudes A_p and A_n from which the $E2$ matrix elements are computed (see the following). For the GXPF1 interaction, these (A_p, A_n) amplitudes, in units of $e\,\mathrm{fm}^2$, have respective values of (8.8,15.4), (10.7,9.5), (9.0,14.4), (10.7,10.6), and (11.8,8.7) for the even $^{48-56}$Ti. The theoretical shell gaps for neutrons at $N = 28, 32$, and 34 result in reduced A_n amplitudes and in excitation spectra for ^{50,54,56}Ti that most closely reflect the $(f_{7/2})^2$ proton structure. The deviation of the experimental ^{56}Ti spectrum from theory indicates a weaker shell gap at $N = 34$. As previously stated, the new GXPF1A interaction [23] improves the agreement, and the new amplitudes $(A_p, A_n) = (10.3, 11.4)$ reflect a larger neutron admixture. With this interaction, the calculated $p_{1/2}$-$f_{5/2}$ shell gap at $N = 34$ is still significant (i.e., 2.5 MeV). Furthermore, this gap is calculated to increase to 3.5 MeV for ^{54}Ca [23], so that a neutron subshell closure is still predicted in this case. The $B(E2, \uparrow)$ rates computed from the (A_p, A_n) values $[B(E2, \uparrow) = (A_p e_p + A_n e_n)^2]$ with conventional effective charges of $e_p = 1.5e$ and $e_n = 0.5e$ overestimate the measured transition rates for the $N = 28$ and 32 nuclei [Table I, Fig. 2(b)]. Moreover, they are rather constant as a function of neutron number, in contrast with the oscillating behavior observed in the experiment. An oscillation related to the neutron shell gaps is present in the A_n amplitudes. It is possible that, for neutron-rich nuclei, the neutron e_n effective charge needs to be increased, while keeping the isoscalar effective charge $e_p + e_n$ constant. Such a modification in the e_p and e_n charges could result in a better agreement with experiment. Recent data [25] on analog states in $A = 51$, $T_z = \pm 1/2$ mirror nuclei suggest that this may well be the case and values of $e_p \sim 1.15e$ and $e_n \sim 0.8e$ were proposed. Although these values would induce a small staggering in the calculated $B(E2)$ values of Fig. 2 (not shown), they are not sufficient to bring experiment and theory in agreement. Additional data on *pf*-shell nuclei are needed to investigate this issue further.

In summary, the present data on absolute $E2$ transition rates, together with earlier work on excitation energies, confirm the presence of a subshell closure at neutron number $N = 32$ in neutron-rich Ti nuclei above ^{48}Ca, an observation in agreement with the results of shell model calculations with the most recent effective interactions. However, the data do not provide any direct indication of the presence of an additional $N = 34$ subshell gap in the Ti isotopes. Moreover, the measured $B(E2; 0^+ \rightarrow 2_1^+)$ probabilities highlight the limitations of the present large-scale calculations as they are unable to reproduce in detail the magnitude of the transition rates in the semimagic nuclei and their strong variation across the neutron-rich Ti isotopes.

The authors thank T. Baumann, A. Stolz, T. Ginter, and M. Steiner and the NSCL cyclotron operations group for providing the secondary and primary beams required for these measurements. This work is supported in part by National Science Foundation Grant Nos. PHY-01-10253, PHY-02-44453, and PHY-98-75122, by the U. S. Department of Energy, Office of Nuclear Physics, under Contracts W–31–109–ENG–38 and DE–FG02–94ER40848, by Grant No. 2PO3B-074-18 of the Polish Scientific Committee, and by the UK Engineering and Physical Sciences Research Council (EPSRC).

[1] B. A. Brown, Prog. Part. Nucl. Phys. **47**, 517 (2001); F. Tondeur, Z. Phys. A **288**, 97 (1978); P. Haensel, J. L. Zdunik, and J. Dobaczewski, Astron. Astrophys. **222**, 353 (1989); J. Dobaczewski, I. Hamamoto, W. Nazarewicz, and J. A. Sheikh, Phys. Rev. Lett. **72**, 981 (1994); J. M. Pearson, R. C. Nayak, and S. Goriely, Phys. Lett. **B387**, 455 (1996); G. A. Lalazissis, D. Vretenar, W. Pöschl, and P. Ring, *ibid.* **B418**, 7 (1998).

[2] T. Otsuka, R. Fujimoto, Y. Utsuno, B. A. Brown, M. Honma, and T. Mizusaki, Phys. Rev. Lett. **87**, 082502 (2001).

[3] A. Huck *et al.*, Phys. Rev. C **31**, 2226 (1985).

[4] R. V. F. Janssens *et al.*, Phys. Lett. **B546**, 55 (2002).

[5] S. N. Liddick *et al.*, Phys. Rev. Lett. **92**, 072502 (2004); Phys. Rev. C **70**, 064303 (2004).

[6] B. Fornal *et al.*, Phys. Rev. C **70**, 064304 (2004).

[7] J. I. Prisciandaro *et al.*, Phys. Lett. **B510**, 17 (2001).

[8] T. Glasmacher, Annu. Rev. Nucl. Part. Sci. **48**, 1 (1998).

[9] G. Kraus *et al.*, Phys. Rev. Lett. **73**, 1773 (1994).

[10] D. C. Radford *et al.*, Phys. Rev. Lett. **88**, 222501 (2002).

[11] M. Honma, T. Otsuka, B. A. Brown, and T. Mizusaki, Phys. Rev. C **65**, 061301 (2002).

[12] D. J. Morrissey *et al.*, Nucl. Instrum. Methods Phys. Res. B **204**, 90 (2003).

[13] D. Bazin *et al.*, Nucl. Instrum. Methods Phys. Res. B **204**, 629 (2003).

[14] W. F. Mueller *et al.*, Nucl. Instrum. Methods Phys. Res. A **466**, 492 (2001).

[15] GEANT, version 3.21, CERN program library, W5013, 1994.

[16] A. Gade *et al.*, Phys. Rev. C **68**, 014302 (2003).

[17] J. Yurkon *et al.*, Nucl. Instrum. Methods Phys. Res. A **422**, 291 (1999).

[18] S. Raman, C. W. Nestor, and P. Tikkanen, At. Data Nucl. Data Tables **78**, 1 (2001).

[19] A. Winther and K. Alder, Nucl. Phys. **A319**, 518 (1979).

[20] C. Zhou, Nucl. Data Sheets **76**, 399 (1995).

[21] B. A. Brown, D. B. Fossan, A. R. Poletti, and E. K. Warburton, Phys. Rev. C **14**, 1016 (1976).

[22] J. Huo, Nucl. Data Sheets **90**, 1 (2000).

[23] M. Honma *et al.*, in Proceedings of the Fourth International Conference on Exotic Nuclei and Atomic Masses (ENAM04) (to be published).

[24] B. Fornal *et al.* (to be published).

[25] R. duRietz *et al.*, Phys. Rev. Lett. **93**, 222501 (2004).